THE JOURNAL OF BIOLOGICAL CHEMISTRY
Vol. 280, No. 29, Issue of July 22, pp. 27093–27102, 2005
© 2005 by The American Society for Biochemistry and Molecular Biology, Inc.
*Printed in U.S.A.*

# A Variable Residue in the Pore of Kv1 Channels Is Critical for the High Affinity of Blockers from Sea Anemones and Scorpions*

Received for publication, December 3, 2004, and in revised form, May 12, 2005
Published, JBC Papers in Press, May 12, 2005, DOI 10.1074/jbc.M413626200

**Bernard Gilquin‡, Sandrine Braud‡, Mats A. L. Eriksson§, Benoît Roux§, Timothy D. Bailey¶, Birgit T. Priest¶, Maria L. Garcia¶, André Ménez‡, and Sylvaine Gasparini‡‖**

*From the ‡Département d'Ingénierie et d'Etudes des Protéines, Commissariat à l'Energie Atomique Saclay, 91191 Gif sur Yvette cedex, France, §Weill Medical College of Cornell University, Department of Biochemistry, New York, New York 10021, and ¶Department of Ion Channels, Merck Research Laboratories, Rahway, New Jersey 07065*

**Animal toxins are associated with well defined selectivity profiles; however the molecular basis for this property is not understood. To address this issue we refined our previous three-dimensional models of the complex between the sea anemone toxin BgK and the S5-S6 region of Kv1.1 (Gilquin, B., Racape, J., Wrisch, A., Visan, V., Lecoq, A., Grissmer, S., Ménez, A., and Gasparini, S. (2002) *J. Biol. Chem.* 277, 37406–37413) using a docking procedure that scores and ranks the structures by comparing experimental and back-calculated values of coupling free energies $\Delta\Delta G_{int}$ obtained from double-mutant cycles. These models further highlight the interaction between residue 379 of Kv1.1 and the conserved dyad tyrosine residue of BgK. Because the nature of the residue at position 379 varies from one channel subtype to another, we explored how these natural mutations influence the sensitivity of Kv1 channel subtypes to BgK using binding and electrophysiology experiments. We demonstrated that mutations at this single position indeed suffice to abolish or enhance the sensitivity of Kv1 channels for BgK and other sea anemone and scorpion toxins. Altogether, our data suggest that the residue at position 379 of Kv1 channels controls the affinity of a number of blocking toxins.**

Molecular recognition and specific association of protein ligands and protein targets are central to most biological processes. Understanding the molecular basis of these interactions is critical for engineering novel protein-protein interactions. In particular, understanding how protein ligands bind with high affinity to only a subset of closely related receptors may help to design ligands with novel selectivities.

A number of studies have been carried out to identify the sites used by protein ligands to bind to several related receptors. These sites were shown to be composed of a core formed by conserved hot spot residues together with target-specific residues (1–5). However, how these sites accommodate the different receptors subtypes is still poorly understood. In many cases the molecular determinants responsible for protein ligand discrimination remain to be identified.

Toxins from sea anemones and scorpions that block currents through Kv1 voltage-gated potassium channels are particularly appropriate to investigate the molecular basis of selectivity of protein-protein interactions since each toxin binds to only a subset of Kv1 channel subtypes (6). We have previously studied in detail BgK, a 37-amino acid peptide isolated from the sea anemone *Bunodosoma granulifera* (7), which binds with similar high affinity to Kv1.1, Kv1.2, and Kv1.6 (8) but not to Kv1.4 and Kv1.5 channels. The sites used by BgK to bind to its different targets were identified by alanine scanning (9). These sites share three critical residues (Lys-25, Tyr-26, and Ser-23), conserved in all Kv1-blocking toxins from sea anemones, which have also been shown to be functional in ShK, another sea anemone toxin (for review, see Ref. 10). Thus, these three residues form the functional core of Kv1-blocking sea anemone toxins. Similarly, a comparison of the functional sites of Kv1-blocking scorpion toxins $\alpha$KTx1–3 (11) suggested a functional core formed by four residues (for review, see Ref. 10). Furthermore, comparison of the functional cores of Kv1-blocking sea anemone and $\alpha$KTx1–3 scorpion toxins revealed that they commonly contain a pair of residues formed by a lysine and a hydrophobic residue (for review, see Ref. 10). This functional dyad (12), which is the smaller common functional denominator of a variety of Kv1-blocking toxins (1), likely reflects a common binding feature of these toxins (10). However, as suggested by a study with a cone snail toxin (13), this binding mode may not be the only one adopted by Kv1-blocking toxins.

Recently, structural models of the complex BgK·S5-S6 region of Kv1.1, based on distance restraints derived from double-mutant cycles (9), revealed that residues from the BgK functional core interact with both conserved and non-conserved residues of Kv1 channels and suggested a role of the latter residues in the selectivity of the toxin for a subset of Kv1 subtypes. In particular, these models emphasized the importance of Kv1.1 residue 379, a variable position in Kv1 channels that is critical for binding of external tetraethylammonium ion (14–17).

In this study we have refined our previous models of the complex BgK·S5-S6 region of Kv1.1 using a previously developed docking procedure (18) that screens the structures by comparing experimental (9) and back-calculated values of coupling free energies $\Delta\Delta G_{int}$ from double-mutant cycles. These models provide a detailed description of the interactions involving the residues of the BgK functional core. Interestingly, one of these interactions, involving the carbonyl of a glycine residue from the channel selectivity filter, appears to be common to the different binding modes used by toxins whether or not they contain a functional dyad. Furthermore, our model strengthens the putative importance of Kv1.1 residue 379. We have investigated the importance of this residue using binding and electrophysiology experiments on different Kv1 channels mutated at position 379. Our results show that mutations at position 379 are sufficient to abolish or enhance sensitivity to toxins, indicating that this single position critically controls the affin-

* The costs of publication of this article were defrayed in part by the payment of page charges. This article must therefore be hereby marked "*advertisement*" in accordance with 18 U.S.C. Section 1734 solely to indicate this fact.

‖ To whom correspondence should be addressed. Tel.: 33-1-69-08-35-88; Fax: 33-1-69-08-90-71; E-mail: sylvaine.gasparini@cea.fr.

ity of BgK and other sea anemone and scorpion toxins for Kv1 channel subtypes.

## EXPERIMENTAL PROCEDURES

*Modeling of the Complex BgK·S5-S6 Region of Kv1.1*—BgK was docked onto a structural model of Kv1.1 using distance restraints derived from double-mutant cycles (9) according to a procedure similar to that developed in Eriksson and Roux (18). The model of Kv1.1 was constructed by using the structure of the bacterial channel KcsA (19) as a template. In addition to the six previously used distance restraints (BgK(Ser-23)-Kv1.1(Tyr-379), BgK(Phe-6)-Kv1.1(Tyr-379), BgK(Tyr-26)-Kv1.1(Ser-357), BgK(Tyr-26)-Kv1.1(Asp-361), BgK(Asn-19)-Kv1.1(Ser-357), BgK-(Tyr-26)-Kv1.1(Tyr-379)) (9), two other restraints were used, BgK(Lys-25N$\zeta$)-Kv1.1(Tyr-375O) and BgK(Phe-6)-Kv1.1(Asp-361). As previously, ambiguous restraints arising from the 4-fold symmetric channel structure were used, but the effective distance was calculated as the distance to the nearest of four equivalent residues (18) instead of using $1/r^6$ sum averaging. The distance restraints were classified as follows: strong, BgK-(Lys-25N$\zeta$)-Kv1.1(Tyr-375O), BgK(Ser-23)–Kv1.1(Tyr-379), and BgK-(Phe-6)-Kv1.1(Tyr-379); medium, BgK(Tyr-26)-Kv1.1(Ser-357), BgK(Tyr-26)-Kv1.1(Asp-361), and BgK(Asn-19)-Kv1.1(Ser-357); weak, BgK(Tyr-26)-Kv1.1(Tyr-379) and BgK(Phe-6)-Kv1.1(Asp-361). A harmonic potential with a flat bottom was used. The upper-bound distances were set to 3, 5, and 6 Å for the strong, medium, and weak restraints, respectively.

The channel was positioned such that the cavity was centered at $z = 0$ and the pore was aligned with the $z$ axis, the extracellular side on the positive side. The atoms of all channel residues for which $z < 10$ were kept fixed. For the other channel residues the backbone atoms were restrained relative to the initial model using a harmonic potential. The strength of the backbone restraints was progressively decreased from 100 to 6 kcal/mol. For the turret residues (residues 345–359), the strength was reduced and decreased from 50 to 0.5 kcal/mol. An energy restraint allowing complete rotation and translation was applied to the toxin backbone (100 kcal/mol) and to the C$\beta$ (10 kcal/mol).

The docking procedure started from a random position and orientation of the toxin. In a first step hydrogen atoms were not included, and electrostatic interactions were ignored. The best structures in terms of van der Waals interaction energy were refined. In a second step hydrogen atoms were introduced, and the system was annealed from 800 to 400 K in 10,000 steps. During these two steps distance restraint force constants were set to 20, 10, 2 kcal/mol for the strong, medium, and weak constraints, respectively. In a final step the structures were refined by slow cooling from 800 to 300 K in 8000 steps during which the distance restraint force constants were reduced to 5, 2, and 0.5 kcal for the strong, medium, and weak constraint, respectively. The equations of motion were integrated using a time step of 2 fs, and the length of all the bonds involving hydrogen atoms were kept rigidly fixed using SHAKE (20). The structures with high levels of energy restraint (>40 kcal/mol) were rejected. The best structures in terms of van der Waals interaction energy were selected. For these structures the $\Delta\Delta G_{int}$ from double-mutant cycles were back-calculated using a continuous implicit solvent model based on the Poisson-Boltzmann equation (18). This equation was solved numerically using the PBEQ module (21) implemented in the program CHARMM (22). A set of atomic Born radii, calibrated and optimized to reproduce the electrostatic free energy of the 20 amino acids in molecular dynamics simulations with explicit water molecules, was used (23). The nonpolar contribution to the binding free energy was empirically written as a fraction of the van der Waals interactions $\lambda\Delta E_{vdW}$ upon formation of the complex, with $\lambda = 0.17$ (18). The dielectric constant of the protein was set to $\epsilon_{prot} = 12$ (18). The structures that gave the best agreement between back-calculated and experimental values (9) were selected. All the calculations were performed using the CHARMM program version c28a3 (22).

*DNAs*—cDNAs encoding hKv1.4, hKv1.5, and hKv1.6, cloned into the mammalian expression vector pcDNA3 (Invitrogen) were kindly provided by Prof. Olaf Pongs (Zentrum für Molekulare Neurobiologie, Hamburg, Germany). cDNAs encoding hKv1.1 and hKv1.3 were cloned into the mammalian expression vector pCI-neo (Promega). The cDNA encoding hKv1.2 in pGEMA was kindly provided by Prof. Stephan Grissmer (Department of Applied Physiology, University of Ulm, Germany) and subcloned into the mammalian expression vector pcDNA3.1/HisC (Invitrogen) as described in (8). Plasmids were amplified in *Escherichia coli* XL1Blue using the plasmid purification kit from Qiagen (maxi protocol). Mutagenesis was performed using the PCR technique (QuikChange™ site-directed mutagenesis kit, Stratagene), and the presence of mutations was confirmed by DNA sequencing of the S5-S6 region.

*Proteins*—BgK and BgK(W5Y/Y26F), an analog that can be radiolabeled without loss of biological activity (8), were synthesized as previously described (8). Synthetic charybdotoxin (ChTX)[1] was purchased from Latoxan (Valence, France), and kaliotoxin (KTX) and ShK were from Bachem (Heidelberg, Germany). Concentrations of BgK and ChTX were obtained by absorbance determination at 280 nm, whereas concentrations of KTX and ShK were assessed from amino acid composition analyses performed on an AminoTag (Jeol). BgK(W5Y/Y26F) was radiolabeled with $^{125}$I as previously described (8).

*Heterologous Expression of Kv1 Channels in Mammalian Cells*—TsA-201 cells were maintained in 10-cm-diameter tissue culture dishes as previously described (8). When near confluency, medium was replaced by antibiotic-free medium, and cells were transfected using 25–30 $\mu$g of DNA and 60 $\mu$l of Lipofectamine 2000 (Invitrogen) according to the manufacturer's instructions. Cells were collected 24 h after transfection, and membranes were prepared as previously described (8).

*Western Blots*—Proteins from membrane preparations were separated on 12.5% SDS-PAGE and transferred to a nitrocellulose membrane (Optitran, Schleicher & Schuell) using a semidry transfer apparatus and Tris-glycine-SDS-methanol buffer. Membranes were saturated overnight at 4 °C with TBS buffer (20 mM Tris-HCl, pH 7.5, 500 mM NaCl) containing 3% (w/v) bovine serum albumin (BSA), washed once with TBS-Tween (0.05% (v/v) Tween 20), and incubated 1 h at room temperature with a rabbit antibody specific for Kv1 subtypes (Sigma) in TBS-Tween buffer containing 0.1% (w/v) BSA. After 3 washes, the membrane was incubated for 1 h at room temperature with a peroxidase-conjugated goat anti-rabbit IgG (Jackson ImmunoResearch), and after three wash steps, the peroxidase reaction was initiated by the addition of 3,3′ diaminobenzidine (Sigma) in 100 mM Tris-HCl, pH 7.4, 0.2% (v/v) $H_2O_2$ to visualize the hybridized probes. Pre-stained molecular weight markers from Biolabs were used.

*Binding Assays*—All binding assays and data analyses were carried out as previously described (8). For measuring dissociation rate constants ($k_{off}$), dissociation was initiated by adding a 4000-fold molar excess of BgK. Aliquots of the binding reaction were diluted at different times into ice-cold wash buffer and filtered as previously described (8).

*Electrophysiology*—For use in automated electrophysiology experiments, Chinese hamster ovary cells maintained in T-75 flasks in Iscove's modified Dulbecco's medium (Invitrogen 12440-046) supplemented with 10% fetal bovine serum (Invitrogen 16000–036), 1% penicillin-streptomycin (Invitrogen 600-5070AG), 2 mM L-glutamine (Invitrogen 320-5030PG), and 1% hypoxanthine-thymidine supplement (Invitrogen 11067-030) in a humidified 5% $CO_2$ incubator at 37 °C were transfected with 2 $\mu$g of DNA using Effectene (Qiagen) and the manufacturer's protocol.

24–48 h after transfection cells were lifted with ~2 ml of Versene (Invitrogen 15040-066) for 6–7 min at 37 °C and suspended in ~10 ml of Dulbecco's phosphate-buffered saline (Mediatech 21-030-CM) containing 2.7 mM KCl, 137 mM NaCl, 15 mM $Na_2HPO_4$, 1.5 mM $KH_2PO_4$, and 0.9 mM $CaCl_2$, 0.5 mM $MgCl_2$. After centrifugation (4 min at ~500 × $g$), the cell pellet was resuspended in 2.5 ml of Dulbecco's phosphate-buffered saline. The intracellular solution consisted of 100 mM potassium gluconate, 40 mM KCl, 3.2 mM $MgCl_2$, 3 mM EGTA, 5 mM HEPES, pH 7.4. Amphotericin B (Sigma A-4888) was prepared as a 40 mg/ml solution in $Me_2SO$ and diluted to 0.13 mg/ml into the internal solution. BgK was prepared in Dulbecco's phosphate-buffered saline.

Kv1.4 and Kv1.5 currents were recorded at room temperature using the IonWorks HT (Molecular Devices) multichannel whole-cell voltage clamp instrument (24). Hole resistances in the planar 384-well electrode array were ~3 megaohms. Electrical access to the cytoplasm was achieved by perforation in 0.13 mg/ml amphotericin B for 4 min. The test pulse consisted of a 150-ms step from a holding potential of −80 mV to +50 mV for Kv1.4 currents and of a 100-ms step from a holding potential of −80 mV to +50 mV followed by 50 ms at −40 mV for Kv1.5 currents. In both cases the pulse was performed before and after 5 min of incubation with BgK, during which the cells were not voltage-clamped, and leak conductances were measured during a 160-ms step from −80 mV to −70 mV preceding the test pulse. Only cells with membrane resistances of >70 megaohms were included in the analysis. Data were acquired at 10 kHz. For mutated Kv1.4 channels, the am-

[1] The abbreviations used are: ChTX, charybdotoxin; $^{125}$I-BgK(W5Y/Y26F), mono-iodotyrosine BgK(W5Y/Y26F); $^{125}$I-HgTX$_1$(A19Y/Y37F), mono-iodotyrosine hongotoxin 1; $K_d$, equilibrium dissociation constant; $K_i$, equilibrium inhibition constant; KTX, kaliotoxin; Kv, voltage-gated potassium (channel); MgTX, margatoxin; r.m.s.d., root mean square deviation.

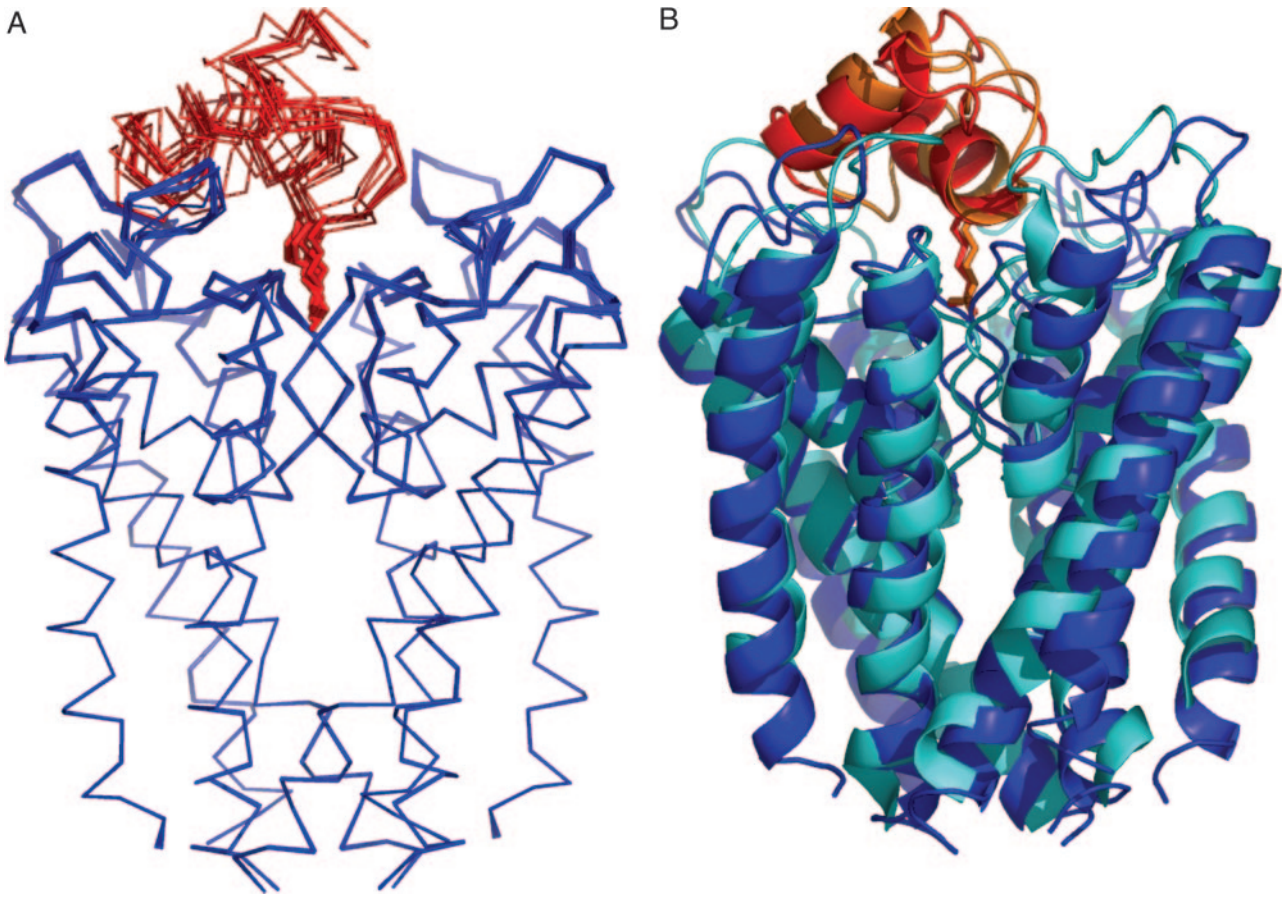


FIG. 1. **Structures of the complexes BgK·S5-S6 region of Kv1.1.** *A*, structures of the eight best complexes (see text). The backbone of BgK and the side chain of residue Lys-25 are colored *red*. The backbone of the S5-S6 region of Kv1.1 is colored *blue*. *B*, comparison of the average structure of the eight structures from (*A*) (BgK, *red*; Kv1.1, *dark blue*) with the average structure from our previous calculations (9) (BgK, *orange*; Kv1.1, *cyan*).

plitude of the peak currents in the presence of BgK was normalized to the peak current in control plotted against peptide concentration and fit to the Hill equation of the form $I_{normalized} = 1/[1 + ([L]/IC_{50})]$, where $[L]$ is the peptide concentration, and $IC_{50}$ is the peptide concentration resulting in 50% inhibition.

## RESULTS

*Refined Model of the BgK·Kv1.1 Complex*—It has been previously shown that values of coupling free energies, $\Delta\Delta G_{int}$, from double-mutant cycles can be calculated from structural models of complexes using a continuum solvent approximation (18). Here, to refine the previous structures of the complex BgK·S5-S6 region of Kv1.1 (9), we implemented a procedure that uses back-calculation of $\Delta\Delta G_{int}$ from double-mutant cycles to screen the model structures (see "Experimental Procedures").

1300 structures were obtained in 9 runs. The best 70, in term of van der Waals interaction energy, were selected. For these structures values of $\Delta\Delta G_{int}$ from double-mutant cycles (9) were back-calculated and compared with the experimental values (Table I). The S.D. between the calculated and measured $\Delta\Delta G_{int}$ varied from 0.6 to 1 kcal/mol. Because of the limited flexibility of the turret region, the distance restraints between BgK(Asn-19)-Kv1.1(Ser-357), BgK(Tyr-26)-Kv1.1(Ser-357), and BgK(Tyr-26)-Kv1.1(Asp-361) were not satisfied, and thus, the values of the corresponding $\Delta\Delta G_{int}$ were close to 0. This reinforces the previous suggestion (25) that the conformation of the turret in the KcsA structure does not reflect the conformation of Kv1 channel turrets. Therefore, we focused on the interactions between Kv1.1(Tyr-379) and BgK residues, for which the S.D. between calculated and experimental $\Delta\Delta G_{int}$ values varied from 0.6 to 1.5 kcal/mol.

For eight of these structures (Table I, Fig. 1*A*), this deviation is less than 0.85 kcal/mol (Fig. 2), and the mean r.m.s.d. for BgK C$\alpha$ around the average structure is 1.3 Å, indicating that localization of BgK is well defined. These structures share several characteristics. First, BgK(Lys-25N$\zeta$) is located between the potassium binding sites S0 and S1 (19, 26). The r.m.s.d. for BgK(K25.C$\alpha$) and BgK(Lys-25N$\zeta$) are equal to 0.8 and 0.5 Å, respectively. Second, the two aromatic rings of BgK residues Tyr-26 and Phe-6 are located between two Kv1.1(Tyr-379) residues from adjacent subunits (r.m.s.d. of C$\alpha$ position of Tyr-26 and Phe-6 is equal to 0.6 and 1.3 Å, respectively). For 5 structures (1–2, 4–5, and 8, Table I), the $\chi$1 of Phe-6 is unchanged, and the value of $\Delta\Delta G_{int}$ for the cycle BgK(F6A)-Kv1.1(Y379H) is positive, as is the experimental value (9). For 2 structures (3 and 7), the $\chi$1 is changed, the BgK(Phe-6) side chain is not in close contact with Kv1.1(Tyr-379), and the value of $\Delta\Delta G_{int}$ for the cycle BgK(F6A)-Kv1.1(Y379H) is negative or zero. Third, in the NMR structures of unbound BgK (12), the side chain of Ser-23 adopts two orientations ($\chi1 \approx -60$ or $+180$). In our calculations a good agreement between back-calculated and experimental $\Delta\Delta G_{int}$ values was obtained only when BgK(Ser-23) was hydrogen-bonded to Kv1.1(Tyr-379) and Kv1.1(Gly-376), implying that the Ser-23 side chain adopts a $\chi$1 close to $-60$. The most frequent hydrogen bonds are those connecting Kv1.1(Tyr-379H$\eta$) to BgK(Ser-23O$\gamma$), Kv1.1(Gly-376O) to BgK(Ser-23H$\gamma$), BgK(Ser-23O$\gamma$) to BgK(Tyr-26HN), and Kv1.1(Gly-376O) to BgK(Lys-25HN). For three structures (2, 4, 8), Kv1.1(Tyr-379) is hydrogen-bonded to the side chain of BgK(Asn-19). For all these complexes, the calculated values of $\Delta\Delta G_{int}$ for the cycle BgK(S23A)-Kv1.1(Y379H) are negative, as is the experimental value (9) (Fig. 2).

TABLE I
*Comparison of experimental and back-calculated values of $\Delta\Delta G_{int}$ for 23 structures*

| Structures | Double-mutant cycle[a] | | | | | | | |
|---|---|---|---|---|---|---|---|---|
| | W5A-Y379H | F6A-Y379H | H13A-Y379H | N19A-Y379H | S23A-Y379H | Q24A-Y379H | K25A-Y379H | Y26A-Y379H |
| | *kcal/mol*$^{-1}$ | | | | | | | |
| Experimental $\Delta\Delta G_{int}$[a] | 0.25 | 1.7 | −0.45 | −0.35 | −1.01 | −0.33 | −2.38 | −0.76 |
| Back-calculated $\Delta\Delta G_{int}$ | | | | | | | | |
| 1 | 0.217 | 0.437 | −0.131 | 0.015 | −0.627 | −0.276 | −1.533 | −0.073 |
| 2 | 0.207 | 0.384 | 0.128 | 0.135 | −0.522 | −0.605 | −1.304 | −0.134 |
| 3 | 0.083 | 0.002 | 0.081 | 0.031 | −0.036 | −0.801 | −2.179 | −0.284 |
| 4 | 0.072 | 0.139 | −0.638 | −0.196 | −0.169 | −0.272 | −1.203 | −1.180 |
| 5 | 0.248 | 0.161 | −0.115 | −0.032 | −0.827 | 0.225 | −1.076 | −0.267 |
| 6 | −0.220 | −0.114 | −0.067 | −0.986 | −0.997 | −0.513 | −1.483 | −0.243 |
| 7 | −0.113 | −0.318 | −0.059 | −0.662 | −1.108 | −0.263 | −1.506 | −0.731 |
| 8 | −0.180 | 0.418 | 0.123 | 0.188 | −0.311 | 0.021 | −0.735 | −0.468 |
| 9 | −0.080 | 0.269 | −0.054 | 0.182 | 0.370 | −0.620 | −1.602 | −0.561 |
| 10 | 0.066 | 0.474 | −0.038 | 0.157 | 0.376 | −0.029 | −1.186 | −0.048 |
| 11 | −0.205 | −0.163 | −0.155 | −0.125 | 0.013 | −0.139 | −1.532 | −0.091 |
| 12 | −0.095 | 0.202 | −0.168 | −0.085 | −0.150 | −1.178 | −1.243 | 0.214 |
| 13 | 0.107 | −0.260 | 0.262 | −0.405 | 0.109 | −0.659 | −1.896 | −0.294 |
| 14 | 0.061 | 0.457 | −0.128 | 0.486 | −0.400 | 0.504 | −0.698 | −0.353 |
| 15 | −0.289 | −0.262 | −0.254 | −0.433 | −0.208 | −0.704 | −1.361 | −0.190 |
| 16 | −0.532 | 0.040 | −0.252 | −0.234 | −1.309 | −0.257 | −0.608 | −0.436 |
| 17 | −0.493 | 0.072 | −0.178 | −0.023 | −0.508 | −0.698 | −0.673 | −0.206 |
| 18 | −0.214 | 0.294 | 0.099 | 0.315 | 0.163 | 0.015 | −0.854 | 0.173 |
| 19 | −0.253 | −0.423 | 0.177 | 0.014 | −0.362 | 0.283 | −1.063 | −0.257 |
| 20 | 0.439 | 0.031 | −0.239 | 0.456 | 0.494 | −0.359 | −1.010 | 0.043 |
| 21 | 0.280 | −0.878 | −0.502 | −0.192 | −0.379 | −0.993 | −1.434 | −0.658 |
| 22 | 0.096 | 0.495 | −0.043 | 0.013 | 0.248 | 0.176 | −0.099 | 0.168 |
| 23 | 0.254 | 0.565 | 0.353 | 0.485 | 0.412 | −0.581 | −0.031 | −0.035 |

[a] Experimental results are from Gilquin *et al.* (9).

Fifteen structures for which the S.D. between back-calculated and experimental $\Delta\Delta G_{int}$ varied from to 0.8 to 1.1 kcal/mol were also examined (Table I). For these complexes, there is no agreement between one or several back-calculated and experimental $\Delta\Delta G_{int}$, and one or several structural characteristics described above are not present. For nine structures (9–11, 13, 15, 18, 20, 22, 23 in Table I), back-calculated $\Delta\Delta G_{int}$ for the cycle BgK(S23A)-Kv1.1(Y379H) is higher than −0.2 kcal/mol, and the hydrogen-bond network around Kv1.1(Tyr-379) and BgK(Ser-23) is reduced to only 1 hydrogen bond. For 5 structures (11, 13, 15, 19, 21) the calculated values of $\Delta\Delta G_{int}$ for the cycle BgK(F6A)-Kv1.1(Y379H) is negative, whereas the experimental value is positive, and BgK(Phe-6) is far from Kv1.1(Tyr-379). For five structures (14, 16, 17, 22, 23), the calculated value of $\Delta\Delta G_{int}$ for the cycle BgK(K25A)-Kv1.1(Y379H) is higher than −0.7 kcal/mol, whereas the experimental value is equal to −2.5 kcal/mol, and in these structures one of the BgK(K25.H$\zeta$) is not hydrogen-bonded with the carbonyl oxygen atoms of the selectivity filter. For one structure (12), BgK(Tyr-26) is not close to Kv1.1(Tyr-379), and the calculated value of $\Delta\Delta G_{int}$ for the cycle BgK(Y26A)-Kv1.1(Y379H) is positive, whereas the experimental value is negative.

In summary, agreement between back-calculated and experimental $\Delta\Delta G_{int}$ values was correlated with two structural characteristics in the complexes. First, BgK(Phe-6) is in close contact to Kv1.1(Tyr-379), and second, Kv1.1(Tyr-379) and BgK(Ser-23) are engaged in a hydrogen-bond network involving BgK(Tyr-26HN), BgK(Lys-25HN), Kv1.1(Gly-376O), and likely BgK(Asn-19O$\delta$1) or BgK(Asn-19N$\delta$2). This is a statistical correlation since only few structures possess all these interactions. To generate a set of structures possessing all these characteristics, complexes were calculated by imposing the following hydrogen bonds: Kv1.1(Tyr-379H$\eta$)-BgK(Ser-23O$\gamma$), Kv1.1(Tyr-379O$\zeta$)-BgK(Asn-19H$\delta$), Kv1.1(Gly-376O)-BgK(Ser-23H$\gamma$), and Kv1.1(Gly-376O)-BgK(Lys-25HN). For the resulting structures there was a good agreement between experimental and back-calculated $\Delta\Delta G_{int}$ for the cycles involving the mutant Kv1.1(Y379H) (average r.m.s.d., 0.78 kcal/mol for the 7 best structures). The hydrogen-bond network obtained is shown in Fig. 3*A*, and the positions of BgK(Tyr-26) and BgK(Phe-6) relative to Kv1.1(Tyr-379) are shown in Fig. 3*B*.

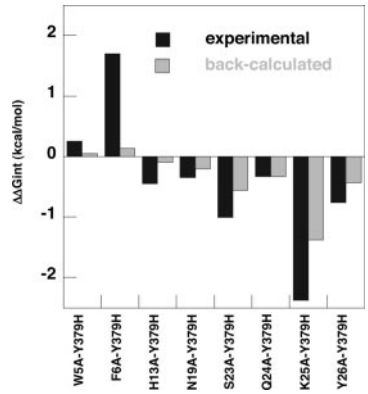


FIG. 2. **Comparison of experimental and back-calculated $\Delta\Delta G_{int}$.** $\Delta\Delta G_{int}$ from double-mutant cycles involving the mutant Kv1.1(Y379H) (9) is shown as *black bars*, and average back-calculated value for the eight best structures of the complexes BgK·S5-S6 region of Kv1.1 are shown as *shaded bars*.

*Position 379 in Kv1 Channels Is Critical for BgK Binding*—The refined models of the complex BgK·S5-S6 region of Kv1.1 strengthen the importance of Kv1.1 residue 379, a variable residue in Kv1 channels (Fig. 4) that was previously suggested to be important for binding of BgK to a subset of Kv1 channel subtypes (8, 9). Indeed, we showed that replacing this single residue in Kv1.3 by the equivalent residue in Kv1.1 (mutant Kv1.3(H399Y)) was sufficient for enhancing BgK affinity by 33-fold, as assessed by competition binding experiments with $^{125}$I-HgTX$_1$(A19Y/Y37F) (8). Furthermore, although no specific binding could be obtained with membranes from tsA-201 cells expressing Kv1.3, the radiolabeled analog of BgK, $^{125}$I-BgK(W5Y/Y26F), could bind to Kv1.3(H399Y) with a $K_d$ of 40 ± 3 pM (Table II) (8).

To further assess the contribution of position 379 as a deter-

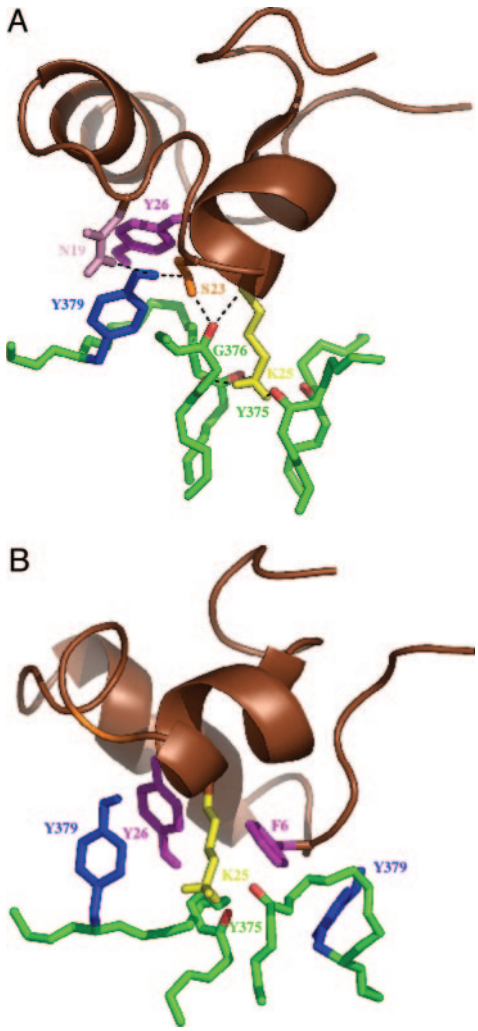


FIG. 3. **Interactions between BgK and Kv1.1 selectivity filter region.** For both *A* and *B*, the Kv1.1 backbone is colored *green*, and the BgK backbone is in *brown*. *A*, hydrogen bond network. The side chains of BgK residues Asn-19, Ser-23, Lys-25, and Tyr-26 are shown. For Kv1.1, the backbone of residues 374–380 and the side chain of Tyr-379 in one subunit, the backbone of residues 374–377 and the oxygen atom of Gly-376 carbonyl (*red*) in the adjacent subunit, the backbone of residues 374–377 in the two other subunits, and the oxygen atom of Tyr-375 carbonyl (*red*) for the four subunits are shown. *B*, positions of residues Tyr-26 and Phe-6 in BgK relative to residues Tyr-379 of Kv1.1 in the complex. For Kv1.1 the backbone of residues 374–380 from two diagonal subunits, the oxygen atom of Tyr-375 carbonyl (*red*) and the side chain of Tyr-379, are shown.

minant of BgK selectivity, we generated Kv1 channels mutated at this position and examined their $^{125}$I-BgK(W5Y/Y26F) binding characteristics using saturation and dissociation kinetics experiments (Fig. 5) (Table II). In addition, since radioactive BgK differs from BgK by two substitutions (W5Y and Y26F) (8), we carried out competition experiments to determine the affinity of BgK for the mutated channels (Table II).

First, we constructed mutants of Kv1.4 and Kv1.5 in which the variable residue corresponding to position 379 in Kv1.1 (Lys and Arg, respectively) was replaced by Tyr or Val, the residues present at that position in Kv1.1 or Kv1.6 and Kv1.2 (Fig. 4). No specific binding of $^{125}$I-BgK(W5Y/Y26F) to membranes from TsA-201 cells expressing wild-type Kv1.4 was observed, whereas binding of $^{125}$I-BgK(W5Y/Y26F) to membranes from cells expressing either Kv1.4(K532V) or Kv1.4(K532Y) was saturable and reversible and displayed $K_d$ values of 340 ± 58 pM ($n$ = 4) and 152 ± 24 pM ($n$ = 3), respectively (Fig. 5, *A* and *C*). Dissociation rate constants, $k_{off}$, were 2.8 ± 0.4 $10^{-2}$ $s^{-1}$ ($n$ = 4) and 1.3 ± 0.2 $10^{-2}$ $s^{-1}$ ($n$ = 5) for Kv1.4(K532V) and Kv1.4(K532Y), respectively (Fig. 5, *B* and *D*). BgK inhibits binding of $^{125}$I-BgK(W5Y/Y26F) to Kv1.4(K532V) and Kv1.4(K532Y), with $K_i$ values of 1120 ± 370 pM ($n$ = 5) and 240 ± 47 pM ($n$ = 7), respectively. Western blots indicated that Kv1.4, Kv1.4(K532Y), and Kv1.4(K532V) are expressed at similar levels, and voltage clamp recordings (see below) showed that the three channels are functional. Thus, we conclude that the absence of $^{125}$I-BgK(W5Y/Y26F) binding to membranes from TsA-201 cells expressing Kv1.4 is not due to lack of expression of the channel and that replacement of Kv1.4 residue Lys-532 by tyrosine or valine is sufficient to confer subnanomolar affinity of $^{125}$I-BgK(W5Y/Y26F) to this channel.

Wild-type Kv1.5 and mutants Kv1.5(R487Y) and Kv1.5(R487V) showed similar expression levels, as indicated by Western blots; a single band corresponding to a 80-kDa protein was revealed in each case (not shown). No specific binding could be observed with wild-type Kv1.5, whereas saturable and reversible binding of $^{125}$I-BgK(W5Y/Y26F) was observed in membranes from cells expressing either Kv1.5(R487Y) or Kv1.5(R487V). These data indicate that replacement of Kv1.5 residue Arg-487 by tyrosine or valine increases the affinity for $^{125}$I-BgK(W5Y/Y26F). However, we were not able to measure these affinities accurately because of very high rates of ligand dissociation (>3 or 5 × $10^{-2}$ $s^{-1}$), which prevented successful separation of free from bound $^{125}$I-BgK(W5Y/Y26F).

Kv1.4 mutants in which residue Lys-532 was replaced by either cysteine or glutamine were previously reported to be functional (27, 28). We constructed these mutants and confirmed by Western blots that they were expressed at similar levels as the wild-type channel (data not shown). Specific binding of $^{125}$I-BgK(W5Y/Y26F) to Kv1.4(K532Q) was not detected. In contrast, $^{125}$I-BgK(W5Y/Y26F) binds to Kv1.4(K532C) channels with a $K_d$ of 94 ± 52 pM ($n$ = 7) (Fig. 5*E*) and with a dissociation rate constant $k_{off}$ of 1.4 ± 0.1 $10^{-2}$ $s^{-1}$ ($n$ = 2) (Fig. 5*F*). BgK inhibits the binding of $^{125}$I-BgK(W5Y/Y26F) to Kv1.4(K532C) with a $K_i$ of 355 ± 142 pM ($n$ = 4).

We then constructed mutants of Kv1.6 in which the variable residue Tyr-429 (Fig. 4) was replaced with either arginine or lysine. Kv1.6 was chosen because of its high affinity for $^{125}$I-BgK(W5Y/Y26F) (Table II). Western blot analysis revealed that expression of wild-type and mutant channels was similar; in all cases a single band corresponding to a 70-kDa protein was detected (data not shown). Specific binding of $^{125}$I-BgK(W5Y/Y26F) could not be detected to either Kv1.6 mutant, indicating that replacement of Kv1.6 residue Tyr-429 by arginine or lysine decreases the affinity for $^{125}$I-BgK(W5Y/Y26F).

Kv1.1 and Kv1.6 mutants were also constructed in which the tyrosine residue was replaced by histidine or valine. For both channels bearing a histidine residue (Kv1.1(Y379H) and Kv1.6(Y429H)), no specific binding of $^{125}$I-BgK(W5Y/Y26F) could be measured, although Western blots indicate that Kv1.6 and Kv1.6(Y429H)) are expressed at similar levels (not shown). Thus, the presence of a histidine residue in Kv1 channels appears to interfere with $^{125}$I-BgK(W5Y/Y26F) binding. When tyrosine is replaced by valine, $^{125}$I-BgK(W5Y/Y26F) binds to the mutated channels with $K_d$ values of 56 ± 16 pM ($n$ = 4) and 17 ± 6 pM ($n$ = 4) for Kv1.1(Y379V) and Kv1.6(Y429V), respectively (Table II). The dissociation rate constants $k_{off}$ are 9.3 ± 0.8 $10^{-3}$ $s^{-1}$ ($n$ = 3) and 4.3 ± 0.5 $10^{-3}$ $s^{-1}$ ($n$ = 4) for Kv1.1(Y379V) and Kv1.6(Y429V), respectively. BgK inhibits the binding of $^{125}$I-BgK(W5Y/Y26F) to Kv1.1(Y379V) and Kv1.6(Y429V), with $K_i$ values of 24 ± 11 pM ($n$ = 3) and 28 ± 14 pM ($n$ = 5), respectively.

Finally, we constructed mutants of Kv1.1 in which Tyr-379 was replaced by serine, threonine, or phenylalanine. Although

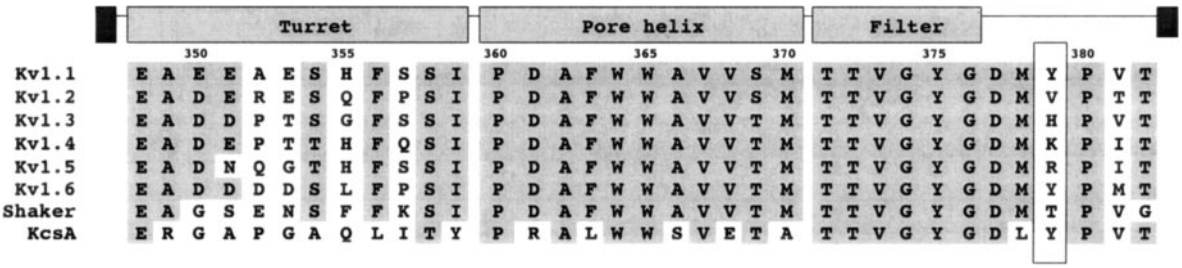


FIG. 4. **Alignment of the amino acid sequences of the S5-S6 regions of Kv1, *Shaker*, and KcsA channels.** Identical or analogous residues are *shaded*. The structural elements derived from the structure of the bacterial *KcsA* channel (19) and residue numbering of Kv1.1 are shown *above* the *sequences*. Position 379 is *boxed*.

TABLE II

*Affinity of $^{125}$I-BgK(W5Y/Y26F) and BgK for native or mutated Kv1 channels*

NSB, no specific binding detected. NMA, non-measurable affinity because of very high dissociation rates.

| Channel | Residue 379[a] | $K_d$ $^{125}$I-BgK(W5Y/Y26F) | $k_{off}$ | $K_i$ BgK[b] | Negatively charged residues in the turret |
|---|---|---|---|---|---|
| | | *pM* | $s^{-1}$ | *pM* | |
| Kv1.1 | Tyr | 35 ± 18[c] | $1.2 \pm 0.1 \times 10^{-2}$ | 18 ± 8 | 4 |
| Kv1.1(Y379V) | Val | 56 ± 16 | $9.3 \pm 0.8 \times 10^{-3}$ | 24 ± 11 | |
| Kv1.1(Y379H) | His | NSB | | | |
| Kv1.1(Y379T) | Thr | 108 ± 32 | $1.2 \pm 0.3 \times 10^{-2}$ | 52 ± 21 | |
| Kv1.1(Y379S) | Ser | NSB | | | |
| Kv1.1(Y379F) | Phe | 29 ± 11 | $4.2 \pm 1.0 \times 10^{-3}$ | 28 ± 8 | |
| Kv1.2 | Val | 77 ± 18[c] | $1.99 \pm 0.01 \times 10^{-2}$ | 49 ± 20 | |
| Kv1.3 | His | NSB | | 777 ± 33[c] | |
| Kv1.3(H399Y) | Tyr | 40 ± 3[c] | $1.9 \pm 0.1 \times 10^{-2}$ | 24 ± 2[c] | 3 |
| Kv1.4 | Lys | NSB | | | |
| Kv1.4(K532Y) | Tyr | 152 ± 24 | $1.3 \pm 0.2 \times 10^{-2}$ | 240 ± 47 | 3 |
| Kv1.4(K532V) | Val | 340 ± 58 | $2.8 \pm 0.4 \times 10^{-2}$ | 1120 ± 370 | |
| Kv1.4(K532Q) | Gln | NSB | | | |
| Kv1.4(K532C) | Cys | 94 ± 52 | $1.4 \pm 0.1 \times 10^{-2}$ | 355 ± 142 | |
| Kv1.5 | Arg | NSB | | | |
| Kv1.5(R487Y) | Tyr | NMA | $>3.5 \times 10^{-2}$ | 765 ± 228 | 2 |
| Kv1.5(R487V) | Val | NMA | $>5 \times 10^{-2}$ | 191 ± 85 | |
| Kv1.6 | Tyr | 4 ± 1[c] | $9.4 \pm 1.3 \times 10^{-4}$ | 16 ± 3 | 5 |
| Kv1.6(Y429V) | Val | 17 ± 6 | $4.3 \pm 0.5 \times 10^{-3}$ | 28 ± 14 | |
| Kv1.6(Y429K) | Lys | NSB | | | |
| Kv1.6(Y429R) | Arg | NSB | | | |
| Kv1.6(Y429H) | His | NSB | | | |

[a] Using Kv1.1 numbering.
[b] Inhibition of $^{125}$I-BgK(W5Y/Y26F) or $^{125}$I-HgTx$_1$(A19Y/Y37F) (Kv1.3 and Kv1.3(H399Y)).
[c] Data are from Racape *et al.* (8).

Western blots indicate that these channels are expressed, no specific binding was obtained with Kv1.1(Y379S). However, $^{125}$I-BgK(W5Y/Y26F) binds to Kv1.1(Y379T) with a $K_d$ of 108 ± 31 pM ($n$ = 5) and to Kv1.1(Y379F) with a $K_d$ of 29 ± 11 pM ($n$ = 6) (Table II), and the dissociation rate constants are $1.2 \pm 0.3\ 10^{-2}$ $s^{-1}$ ($n$ = 3) and $4.2 \pm 1\ 10^{-3}$ $s^{-1}$ ($n$ = 4) for Kv1.1(Y379T) and Kv1.1(Y379F), respectively. BgK inhibits the binding of $^{125}$I-BgK(W5Y/Y26F) to Kv1.1(Y379F) and Kv1.6(Y429T), with $K_i$ values of 28 ± 8 pM ($n$ = 5) and 52 ± 21 pM ($n$ = 5), respectively.

*BgK Blocks Mutated Kv1.4 and Kv1.5 Channels*—The ability of BgK to block currents through different Kv1 channels was investigated using automated electrophysiology (see "Experimental Procedures"). Although 1 μM BgK has no significant inhibitory activity on Kv1.4 channels expressed in Chinese hamster ovary cells, it blocks 92 ± 2% ($n$ = 9) and 85 ± 6% ($n$ = 5) of currents through Kv1.4(K532V) and Kv1.4(K532Y) channels, respectively (Fig. 6). Dose-response curves were established to block of the mutated channels (Fig. 6); BgK blocks both mutants with similar potency ($IC_{50}$ of 87 and 84 nM for Kv1.4(K532V) and Kv1.4(K532Y), respectively). Similarly, 5 μM BgK has no significant inhibitory activity on Kv1.5 channels expressed in Chinese hamster ovary cells, whereas 500 nM BgK blocks 73 ± 25% ($n$ = 13) and 60 ± 15% ($n$ = 10) currents through Kv1.5(R487V) and Kv1.5(R487Y) channels, respectively (Fig. 6), indicating that the $IC_{50}$ values of BgK for these channels are close to 500 nM. For comparison, we previously showed that BgK blocks Kv1.2 with an $IC_{50}$ of 22.9 nM (29).

*Kv1 Channel Position 379 Is Critical for Binding of Other Toxins*—Competition experiments were carried out to measure the ability of two scorpion toxins, ChTX (αKTx1.1) and KTX (αKTx3.1) (11), to inhibit $^{125}$I-BgK(W5Y/Y26F) binding to different Kv1 channels bearing either a valine or a tyrosine residue at position 379 (Table III). We found that ChTX binds with 2 or 3 orders of magnitude higher affinity to channels possessing a valine residue than to channels possessing a tyrosine residue. Reciprocally, KTX binds with 2 orders of magnitude higher affinity to channels possessing a tyrosine residue than to channels possessing a valine residue. These results agree with previous studies carried out with mutated Kv1.3 channels (30, 31). Furthermore, both toxins are able to bind with nM affinity to Kv1.4 channels bearing a single mutation (Kv1.4(K532V) for ChTX and Kv1.4(K532Y) for KTX) (Table III).

We also assessed the ability of the sea anemone toxin ShK to inhibit $^{125}$I-BgK(W5Y/Y26F) binding to Kv1.4(K532V) and Kv1.4(K532Y) (Table III). Although this toxin does not block Kv1.4 channels (32), it inhibits $^{125}$I-BgK(W5Y/Y26F) binding to Kv1.4(K532V) and Kv1.4(K532Y) (Table III). Furthermore, it binds to channels possessing a tyrosine residue with 60-fold higher affinity than to channels possessing a valine residue.

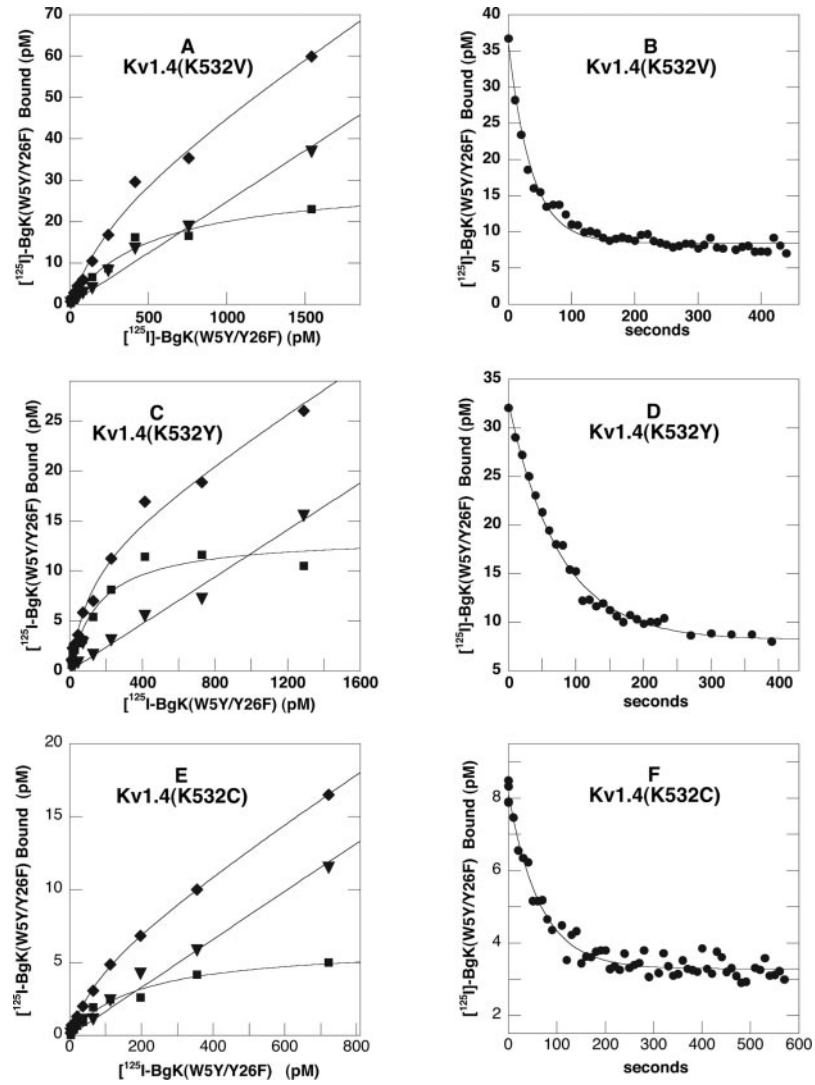


FIG. 5. **Binding of $^{125}$I-BgK(W5Y/Y26F) to mutated Kv1.4 channels.** *A*, *C*, and *E*, saturation binding experiments. Membranes prepared from TsA-201 cells expressing either Kv1.4(K532V) (*A*), Kv1.4(K532Y) (*C*), or Kv1.4(K532C) (*E*) channels were incubated with increasing concentrations of $^{125}$I-BgK(W5Y/Y26F) in a total volume of 600 $\mu$l (*A* and *C*) or 500 $\mu$l (*E*), as indicated under "Experimental Procedures." Nonspecific binding (▼) was determined in the presence of 300 nM (*A* and *E*) or 170 nM (*C*) BgK. Specific binding (■) was assessed from the difference between total binding (♦) and nonspecific binding (▼). *A*, $K_d$ Kv1.4(K532V) = 334 pM, $B_{max}$ = 26.7 pM. *C*, $K_d$ Kv1.4(K532Y) = 116 pM, $B_{max}$ = 12.6 pM. *E*, $K_d$ Kv1.4(K532C) = 94 pM, $B_{max}$ = 5 pM. *B*, *D*, and *F*, dissociation kinetics. Membranes were incubated with 95 pM (*B*) 165 pM (*D*), or 105 pM (*F*) $^{125}$I-BgK(W5Y/Y26F). When equilibrium was reached, a 4000-fold molar excess of BgK was added, and bound ligand was determined at different time points as described under "Experimental Procedures." *B*, $k_{off}$ = 2.75 $10^{-2}$ $s^{-1}$. *D*, $k_{off}$ = 1.32 $10^{-2}$ $s^{-1}$. *F*, $k_{off}$ = 1.52 $10^{-2}$ $s^{-1}$.

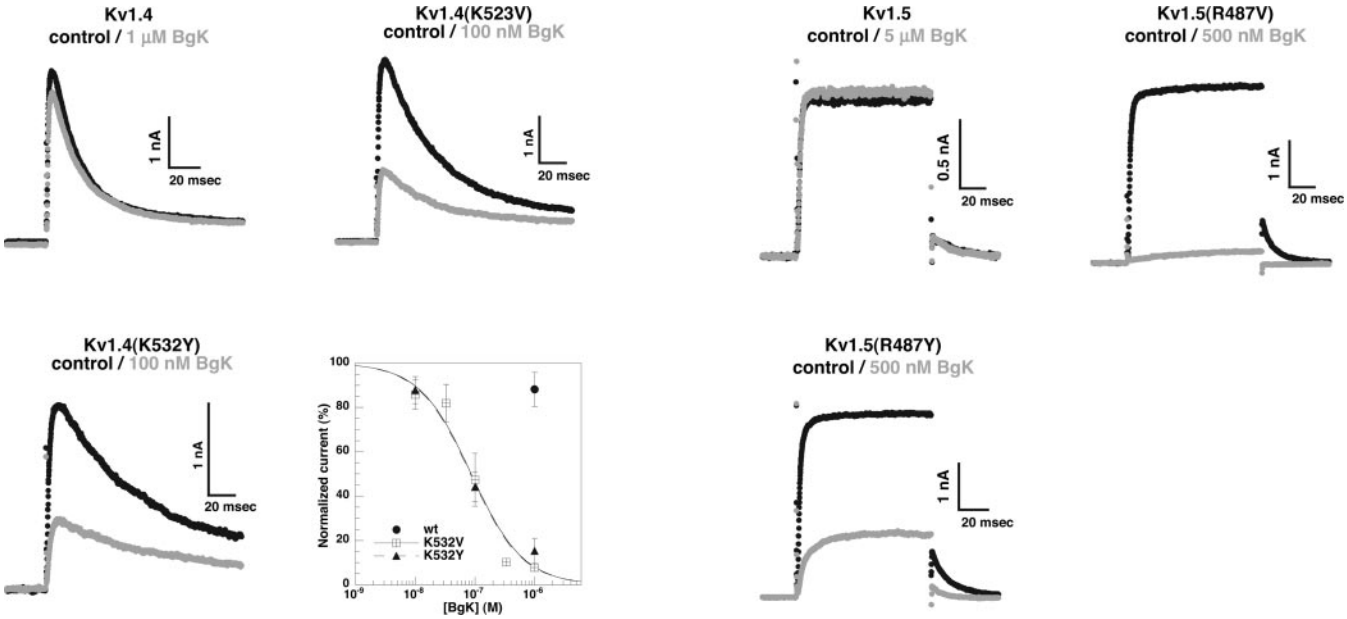


FIG. 6. **Block by BgK of currents through Kv1.4 and Kv1.5 mutant channels expressed in Chinese hamster ovary cells.** Kv1.4 (*left*) and Kv1.5 (*right*) currents were recorded in control and 5 min after application of BgK, as indicated. Kv1.4 currents were activated by a 150-ms step from a holding potential of −80 mV to +50 mV, and Kv1.5 currents were activated by a 100-ms step from −80 mV to +50 mV followed by 50 ms at −40 mV. For the dose-response curve, mean values were calculated from 3 to 13 determinations, except only one determination was made for 33 nM BgK applied to Kv1.4(K532V). Currents in BgK are plotted as % of control currents. The $IC_{50}$ values determined were 87 nM for Kv1.4(K532V) and 84 nM for Kv1.4(K532Y). *wt*, wild type.

TABLE III

*Affinity of sea anemone toxins BgK and ShK and scorpion toxins ChTX and KTX for Kv1 channels possessing either a tyrosine or a valine residue at position 379*

ND, not determined.

| Residue 379[a] | $K_i$[b] | | | | | | |
|---|---|---|---|---|---|---|---|
| | Kv1.1 Tyr | Kv1.1(Y379V) Val | Kv1.2 Val | Kv1.4(K532Y) Tyr | Kv1.4(K532V) Val | Kv1.6 Tyr | Kv1.6(Y429V) Val |
| | | | | | *nM* | | |
| BgK | 18 ± 8 pM | 24 ± 11 pM | 49 ± 20 pM | 240 ± 47 pM | 1.1 ± 0.4 nM | 16 ± 3 pM | 28 ± 14 pM |
| ShK | ND | ND | ND | 72 ± 32 pM | 4.2 ± 1.0 nM | ND | ND |
| KTX | 92 ± 6 pM | 11 ± 4 nM | 1.4 ± 0.6 nM | 15 ± 3 nM | 646 ± 363 nM | 2.7 ± 1.3 pM | 179 ± 54 pM |
| ChTX | 101 ± 18 nM[c] | 154 ± 95 pM | 34 ± 10 pM | 348 ± 170 nM | 1.8 ± 0.9 nM | 74 ± 5 nM | 13 ± 6 pM |

[a] Using Kv1.1 numbering.
[b] Inhibition of $^{125}$I-BgK(W5Y/Y26F) binding to membranes from transfected TsA-201 cells.
[c] Data are from Racape *et al.* (8).

## DISCUSSION

One of the main goals of studying protein-protein interactions is to understand the molecular basis of selectivity or, in other words, how a protein ligand can display large differences in affinity for closely related receptors. Sea anemone and scorpion toxins αKTx1–3 that block Kv1 voltage-gated potassium channels offer a well documented model system to address this issue. Indeed, these toxins bind with high affinity to different subsets of Kv1 channels, and none of them bind to Kv1.4 and Kv1.5 channels (Refs. 6 and 32 and this study). It was previously shown that association of these toxins with their different targets is mediated by residues from a conserved functional core and by variable target-specific residues (for review, see Refs. 1 and 10). Furthermore, the presence in the functional cores of these toxins of a common denominator formed by two residues (the functional dyad) suggests that toxins sharing this feature have undergone convergent evolution, with the dyad acting as a common anchor in each complex (9, 12) (for review, see Ref. 10). However, although these toxins possess such a similar binding anchor, they display distinct selectivity toward the different Kv1 channels subtypes, and the molecular features responsible for these distinct profiles of selectivity are not yet understood.

In the current study we addressed the above issue by establishing refined models of the complex between the sea anemone toxin BgK and the S5-S6 region of Kv1.1. These models were generated with a procedure (18) that screens the structures by back-calculating the $\Delta\Delta G_{int}$ from double-mutant cycles. This approach led us with well defined complex structures with a r.m.s.d. of 1.3 Å around the average BgK position. The average distance between BgK Cα of mean structures from this procedure and the previous one (9) is 3.0 Å but is reduced to 1 Å for the functional core residues of BgK (Lys-25, Tyr-26, and Ser-23). The interactions involving these residues were determined in more detail with this procedure since, in addition to those previously determined for the functional dyad residues Lys-25 and Tyr-26 of BgK (9), it identified interactions between the third residue of the BgK functional core (Ser-23) and Kv1.1 residues Tyr-379 and Gly-376.

Therefore, the interactions involving the BgK functional core residues appear to be of two types. Some involve the main-chain atoms of the channel and, thus, may be conserved in each complex. They correspond to previously described interactions between the dyad lysine side chain and the carbonyl oxygen atoms of the selectivity filter (9) and to hydrogen bonds between the Ser-23 side chain and the carbonyl oxygen atoms of Gly-376. Interestingly, a recent study based on molecular docking (33) identified interactions between the conserved functional residue Ser-10 of scorpion toxins from subfamilies αKTx1 and αKTx3 (11) and the carbonyl of Kv1.3(Gly-396), equivalent to Kv1.1(Gly-376). Furthermore, a very recent model of the complex (34) between the cone snail κM-conotoxin RIII-K that does not contain a functional dyad (13), and the TSha1 channel, a Kv1 channel from the rainbow trout, identified a similar interaction between the side chain of the hydroxyproline O15 from the toxin and the carbonyl of TSha1(Gly-373), equivalent to Kv1.1(Gly-376). Therefore, this interaction appears to be common to the binding of toxins whether or not they possess a functional dyad. The second interactions involving the binding core residues of BgK are established with the side chain of a variable residue of Kv1 channels (Tyr-379 in Kv1.1). This residue interacts with the aromatic residues Tyr-26 (from the dyad) and Phe-6, and the spatial organization of these aromatic rings is frequently conserved in proteins (35). The side chain of Tyr-379 also forms hydrogen bonds with the side chain of the BgK binding core residue Ser-23 and with Asn-19.

That the binding core residues of BgK interact with a non-conserved residue of the channel suggested a critical role of the position of this channel for BgK selectivity (9). We further investigated this idea by determining the affinity of BgK and $^{125}$I-BgK(W5Y/Y26F), a radiolabeled analog of BgK (8), for different Kv1 channels mutated at that position using binding and electrophysiology experiments. Although our experiments did not formally rule out that the absence of specific binding with some mutated channels could be due to other reasons than low affinity of $^{125}$I-BgK(W5Y/Y26F), such as lack of channel tetramerization, we believe that this is unlikely to be the case since most of these mutated channels (Kv1.1(Y379H), Kv1.6(Y429K), Kv1.4(K532Q)) have been previously shown to be functional (28, 36, 37). Position 379 of Kv1 channels appears to be a critical determinant for BgK binding since mutations at this position are sufficient to alter the affinity for BgK. Thus, we could generate Kv1.4 and Kv1.5 channels sensitive to $^{125}$I-BgK(W5Y/Y26F) and BgK by solely introducing a valine or a tyrosine at this position. In the complex BgK·S5-S6 region of Kv1.1, Tyr-379 establishes both hydrophobic interactions with BgK residues Phe-6 and Tyr-26 and hydrogen bonds with residues Ser-23 and Asn-19. However, our results indicate that these hydrogen interactions are not critical since replacing Tyr-379 in Kv1.1 by phenylalanine does not reduce the affinity for BgK. Furthermore, we found that all the residues at position 379 that could confer high affinity to $^{125}$I-BgK(W5Y/Y26F) and BgK (Tyr, Phe, Thr, Val, Cys) allow hydrophobic interactions. Therefore, in agreement with our previous suggestion (9), the hydrophobic component of the interactions involving residues at position 379 is likely to be critical for BgK to bind Kv1 channels with high affinity.

Previous studies have shown that position 379 is also important for scorpion toxins since agitoxin does not bind to *Shaker*

channels containing lysine or glutamine residues at this position (449, using Shaker numbering) (38), and ChTX, KTX, and margatoxin (MgTX) do not bind to Kv1.3 channels containing arginine residue at this position (30). In our study we also demonstrated that this position is an essential component for high affinity binding of the scorpion toxins ChTX and KTX and the sea anemone peptide ShK. Altogether, these results indicate that position 379 is critical for the selectivity of sea anemone and scorpion toxins and differentiates between two groups of Kv1 channels. First, the channels possessing a lysine, arginine, or glutamine residue at position 379, such as Kv1.4 and Kv1.5, are not recognized by these toxins. Second, channels possessing a valine, tyrosine, phenylalanine, threonine, histidine, or cysteine residue at position 379 bind some of these toxins. However, a number of these toxins can bind to only a subset of channels from this second group, and again, it seems that this selectivity is dictated by the nature of the residue at position 379. Thus, the low affinity of BgK for Kv1.3 and of ShK for Kv1.2 channels (39) seems to reflect the presence in these channels of a histidine and a valine residue, respectively, whereas the low affinity of ChTX for Kv1.1 channels (8) seems to reflect the presence of a tyrosine residue. Moreover, it was recently shown that this position also contributes significantly to the selectivity of the scorpion toxin maurotoxin (40). Therefore, each toxin seems to "sense" the nature of the side chain of residue 379 in a unique way.

Other proteins also bind to their different targets using highly conserved residues that form a "functional core" and target-specific variable residues (2–5). This binding mode, called "two components binding mode" (1) or "dual recognition" (2, 3), has been described in large detail for bacterial immunity proteins, which bind with high affinity to cognate colicins and with low affinity to non-cognate colicins (2, 3). It was shown that two of the three conserved hot spot residues of the functional core of immunity proteins interact with a variable residue of colicins and that the high affinity of a immunity protein for its cognate colicin is conferred by the capacity of some of its variable residues to interact with this colicin variable residue (2, 3). Data reported in this paper also suggest a similar mechanism for toxins; the high affinity of a toxin for a particular Kv1 subtype could be conferred by the capacity of target-specific variable residues to interact with the variable channel residue at position 379. Two main arguments support this hypothesis. First, BgK(Phe-6), a target-specific residue (9), is in close contact to Kv1.1(Tyr-379). Second, ShK, a sea anemone toxin homolog to BgK, can bind to Kv1.3 with high affinity, whereas BgK cannot, and it was shown that ShK(Arg-11), a residue absent in BgK, interacts with Kv1.3(His-404), the equivalent residue in the channel to Kv1.1(Tyr-379) (41).

Obviously, residue 379 is not the only determinant for toxin selectivity, and other Kv1 channel regions may have some influence since a toxin does not necessarily bind with the same affinity to channels possessing the same residue in position 379. For instance, the scorpion toxin hongotoxin 1 binds to Kv1.6 with an affinity 2 orders of magnitude lower than to Kv1.1 (42). For BgK, there seems to be a correlation between the charge of the turret and the kinetics of dissociation of $^{125}$I-BgK(W5Y/Y26F), which are slower when the turret contains more negatively charged residues. This was inferred from comparison of $^{125}$I-BgK(W5Y/Y26F) dissociation rates for the channels Kv1.1, Kv1.3(H399Y), Kv1.4(K532Y), and Kv1.6, which all possess a tyrosine residue in position 379 and whose S5-S6 regions differ by the position 381, which is uncharged in all cases, and by their turret sequences and charges. Also, it was shown that the turret region influences ChTX binding since a single mutation in the *Shaker* channel turret increases its affinity by 3 orders of magnitude (43).

In conclusion, we demonstrated that position 379 is critical for the selectivity of BgK and other toxins possessing a functional dyad. This suggests that this residue could be a major actor in the "two binding components" or "dual recognition" of Kv1 channels by these toxins by interacting with both conserved residues from the functional core of the toxin and target-specific variable residues.

*Acknowledgment*—We are grateful to Antony Caruana for technical assistance.

REFERENCES

1. Ménez, A., Servent, D., and Gasparini, S. (2002) in *Pespectives in Molecular Toxinology* (Ménez, A., ed) pp. 175–200, John Wiley & Sons, Inc., Chichester, UK
2. Li, W., Keeble, A. H., Giffard, C., James, R., Moore, G. R., and Kleanthous, C. (2004) *J. Mol. Biol.* **337,** 743–759
3. Kuhlmann, U. C., Pommer, A. J., Moore, G. R., James, R., and Kleanthous, C. (2000) *J. Mol. Biol.* **301,** 1163–1178
4. Zhang, Z., and Palzkill, T. (2004) *J. Biol. Chem.* **279,** 42860–42866
5. Zhang, Z., and Palzkill, T. (2003) *J. Biol. Chem.* **278,** 45706–45712
6. Kaczorowski, G. J., and Garcia, M. L. (1999) *Curr. Opin. Chem. Biol.* **3,** 448–458
7. Cotton, J., Crest, M., Bouet, F., Alessandri, N., Gola, M., Forest, E., Karlsson, E., Castaneda, O., Harvey, A. L., Vita, C., and Menez, A. (1997) *Eur. J. Biochem.* **244,** 192–202
8. Racape, J., Lecoq, A., Romi-Lebrun, R., Liu, J., Kohler, M., Garcia, M. L., Menez, A., and Gasparini, S. (2002) *J. Biol. Chem.* **277,** 3886–3893
9. Gilquin, B., Racape, J., Wrisch, A., Visan, V., Lecoq, A., Grissmer, S., Ménez, A., and Gasparini, S. (2002) *J. Biol. Chem.* **277,** 37406–37413
10. Gasparini, S., Gilquin, B., and Menez, A. (2004) *Toxicon* **43,** 901–908
11. Tytgat, J., Chandy, K. G., Garcia, M. L., Gutman, G. A., Martin-Eauclaire, M. F., van der Walt, J. J., and Possani, L. D. (1999) *Trends Pharmacol. Sci.* **20,** 444–447
12. Dauplais, M., Lecoq, A., Song, J., Cotton, J., Jamin, N., Gilquin, B., Roumestand, C., Vita, C., de Medeiros, C. L., Rowan, E. G., Harvey, A. L., and Menez, A. (1997) *J. Biol. Chem.* **272,** 4302–4309
13. Al-Sabi, A., Lennartz, D., Ferber, M., Gulyas, J., Rivier, J. E., Olivera, B. M., Carlomagno, T., and Terlau, H. (2004) *Biochemistry* **43,** 8625–8635
14. Kavanaugh, M. P., Varnum, M. D., Osborne, P. B., Christie, M. J., Busch, A. E., Adelman, J. P., and North, R. A. (1991) *J. Biol. Chem.* **266,** 7583–7587
15. MacKinnon, R., and Yellen, G. (1990) *Science* **250,** 276–279
16. Liman, E. R., Tytgat, J., and Hess, P. (1992) *Neuron* **9,** 861–871
17. Heginbotham, L., LeMasurier, M., Kolmakova-Partensky, L., and Miller, C. (1999) *J. Gen. Physiol.* **114,** 551–560
18. Eriksson, M. A., and Roux, B. (2002) *Biophys. J.* **83,** 2595–2609
19. Zhou, Y., Morais-Cabral, J. H., Kaufman, A., and MacKinnon, R. (2001) *Nature* **414,** 43–48
20. Ryckaert, J. P., Ciccotti, G., and Berendsen, H. J. C. (1977) *J. Comput. Phys.* **23,** 327–341
21. Im, W., Beglov, D., and Roux, B. (1998) *Comput. Phys. Commun.* **111,** 59–75
22. Brooks, B. R., Bruccoleri, R. E., Olafson, B. D., States, D. J., Swaminathan, S., and Karplus, M. (1983) *J. Comput. Chem.* **4,** 187–217
23. Nina, M., Beglov, D., and Roux, B. (1997) *J. Phys. Chem. B* **101,** 5239–5248
24. Schroeder, K., Neagle, B., Trezise, D. J., and Worley, J. (2003) *J. Biomol. Screen.* **8,** 50–64
25. Wrisch, A., and Grissmer, S. (2000) *J. Biol. Chem.* **275,** 39345–39353
26. Berneche, S., and Roux, B. (2001) *Nature* **414,** 73–77
27. Claydon, T. W., Boyett, M. R., Sivaprasadarao, A., Ishii, K., Owen, J. M., O'Beirne, H. A., Leach, R., Komukai, K., and Orchard, C. H. (2000) *J. Physiol.* (*Lond.*) **526,** 253–264
28. Claydon, T. W., Boyett, M. R., Sivaprasadarao, A., and Orchard, C. H. (2002) *Am. J. Physiol. Cell Physiol.* **283,** 1114–1121
29. Braud, S., Belin, P., Dassa, J., Pardo, L., Mourier, G., Caruana, A., Priest, B. T., Dulski, P., Garcia, M. L., Menez, A., Boulain, J. C., and Gasparini, S. (2004) *Protein Expression Purif.* **38,** 69–78
30. Aiyar, J., Withka, J. M., Rizzi, J. P., Singleton, D. H., Andrews, G. C., Lin, W., Boyd, J., Hanson, D. C., Simon, M., Dethlefs, B., Lee, C., Hall, J. E., Gutman, G. A., and Chandy, K. G. (1995) *Neuron* **15,** 1169–1181
31. Aiyar, J., Rizzi, J. P., Gutman, G. A., and Chandy, K. G. (1996) *J. Biol. Chem.* **271,** 31013–31016
32. Beeton, C., Wulff, H., Singh, S., Botsko, S., Crossley, G., Gutman, G. A., Cahalan, M. D., Pennington, M., and Chandy, K. G. (2003) *J. Biol. Chem.* **278,** 9928–9937
33. Gao, Y. D., and Garcia, M. L. (2003) *Proteins* **52,** 146–154
34. Verdier, L., Al-Sabi, A., Rivier, J. E. F., Olivera, B. M., Terlau, H., and Carlomagno, T. (2005) *J. Biol. Chem.* **280,** 21246–21255
35. Burley, S. K., and Petsko, G. A. (1985) *Science* **229,** 23–28
36. Hurst, R. S., Busch, A. E., Kavanaugh, M. P., Osborne, P. B., North, R. A., and Adelman, J. P. (1991) *Mol. Pharmacol.* **40,** 572–576
37. Gomez-Hernandez, J. M., Lorra, C., Pardo, L. A., Stuhmer, W., Pongs, O., Heinemann, S. H., and Elliott, A. A. (1997) *Pfluegers Arch. Eur. J. Physiol.* **434,** 661–668
38. MacKinnon, R., Heginbotham, L., and Abramson, T. (1990) *Neuron* **5,** 767–771
39. Middleton, R. E., Sanchez, M., Linde, A. R., Bugianesi, R. M., Dai, G., Felix,

J. P., Koprak, S. L., Staruch, M. J., Bruguera, M., Cox, R., Ghosh, A., Hwang, J., Jones, S., Kohler, M., Slaughter, R. S., McManus, O. B., Kaczorowski, G. J., and Garcia, M. L. (2003) *Biochemistry* **42,** 13698–13707
40. Visan, V., Fajloun, Z., Sabatier, J. M., and Grissmer, S. (2004) *Mol. Pharmacol.* **66,** 1103–1112
41. Kalman, K., Pennington, M. W., Lanigan, M. D., Nguyen, A., Rauer, H., Mahnir, V., Paschetto, K., Kem, W. R., Grissmer, S., Gutman, G. A., Christian, E. P., Cahalan, M. D., Norton, R. S., and Chandy, K. G. (1998) *J. Biol. Chem.* **273,** 32697–32707
42. Koschak, A., Bugianesi, R. M., Mitterdorfer, J., Kaczorowski, G. J., Garcia, M. L., and Knaus, H. G. (1998) *J. Biol. Chem.* **273,** 2639–2644
43. Goldstein, S. A., and Miller, C. (1992) *Biophys. J.* **62,** 5–7